Modelling and Preliminary Design Issues of a 4-Axis Parallel Machine for Heavy Parts Handling

O. Company, S. Krut and **F. Pierrot**[1]

LIRMM, UMR5506 CNRS - Université Montpellier II

161, rue Ada 34392 Montpellier Cedex 5, France

Abstract: This paper presents a new 4 degree of freedom parallel mechanism dedicated to handling of heavy parts within a large workspace. These 4 degrees of freedom are 3 translations and 1 rotation about a given axis. Such a mechanism is rare because most of common parallel mechanisms have 3 or 6 degrees of freedom. Firstly, a description of the mechanism is given. Then models are derived regarding velocity and force transformation as input-output relationship. Finally, internal forces models and stiffness model are evaluated. All models are embedded in a software module aiming to help with preliminary design of machines based on this new architecture.

Keywords: parallel kinematics mechanism, design, input/output laws, accuracy, stiffness

[1] corresponding author: François Pierrot,

LIRMM, 161 rue Ada 34392 Montpellier cedex 5 – France

Tel: +33 467 418 604, email: pierrot@lirmm.fr

NOTATION

$\mathbf{I_3}$	Identity matrix of rank 3
pre*(X)*	pre-cross-product matrix associated to vector $\boldsymbol{X}$
$\mathbf{Rot}(\boldsymbol{W},q)$	rotation matrix describing the rotation of angle q about $\boldsymbol{W}$

1 INTRODUCTION

The first parallel mechanism was designed by Gough in 1957 for pneumatics testing [**1**] and in the mid 80's the three degree-of-freedom Delta robot designed by Clavel [**2**] proved the efficiency of well designed parallel mechanisms for high-speed, small-object applications (see [**3**] for a review of existing parallel mechanisms). Recently, a fast machine-tool based on the same concept, Urane Sx [**4**], has been built and its performances are a *3.5g* guaranteed acceleration on the whole workspace (with up *to 5.0g* for a sub part of the workspace). So, parallel mechanisms are a good choice to achieve very fast operations, and both machining and robotics fields already appreciated their efficiency. This paper attends to show that parallel mechanisms could also be used to build fast handling machines where until nowadays only gantry-like devices are used. The case study presented in this paper regards handling machines for heavy parts (more than *100 kg*) such that parts handled in automotive and truck industry: crankshafts, flywheels, cylinder heads, etc.

It is well known that parallel and serial mechanisms have, by construction, opposite characteristics [**5**], and that the main drawback of parallel mechanisms is their small workspace compare to serial machines, in particular concerning the orientation range of their end point. Typically a mean value of the tilting angle for a Gough platform is 15° [**6**] witch is not enough to achieve numerous tasks. Different solutions are possible to suppress this drawback:

- To build hybrid parallel/serial mechanisms like Neos Robotics Tricept architecture [**7**]. This architecture is composed by a parallel mechanism (three active chains, plus a passive chain) carrying a 2 or 3-degree-of-freedom wrist. Such an architecture is used for both robotic tasks and machining.
- To build machines based on the *Right Hand / Left Hand* paradigm, that is to say that both tool and manufactured part move with respect to the ground.
- To build redundant mechanisms, that is to say over-actuated, like the Sena Technologie Eclipse [**8**] machine tool or the Archi robot [**9**] developed at LIRMM. The Eclipse machine tool is designed to achieve five faces milling; the Archi robot is a planar 3 degree-of-freedom robot with unlimited rotation capability.
- To add amplification systems at the wrist level to increase the range of tool orientation.

For the considered application – handling of heavy parts – 4 degrees of freedom are needed: three translation to move the part from point to point, one rotation (often about a vertical axis) to orient it. In some regards, this can be seen as very similar to pick-and-place; however two key characteristics of handling applications are really specific: (i) parts are heavier than in pick-and-place applications (more than *100 kg*, compared to a typical *1 kg* object), (ii) the workspace is larger and often has one dimension that is dramatically different from the others. For example, in this paper, numerical studies will concern *116 kg* parts and a *3.0m*x*0.5m*x*0.5m* workspace (with a complete rotation about the vertical axis).

Most of existing parallel mechanisms and robots have 3 or 6 degrees of freedom. Only very few have 4 degrees of freedom [**10**] [**11**] [**12**] [**13**] [**14**], and none of them offer the 3-translation, 1-rotation combination needed for handling. Even the Delta with its additional, non-parallel, fourth degree of freedom cannot fulfil the requirements: it is not possible to add such a telescopic passive chain for a several-meter long workspace.

The aim of this paper is to present a mechanism that provides the needed 4 degrees of freedom (3 translations and 1 rotation about a given axis) and then to study it in details. After a short description of its mechanical architecture, geometry and kinematics modelling are presented. Then forces transmission between actuators and nacelle as well as internal forces models are. A simplified stiffness analysis and an accuracy study are also carried out. To offer numerical examples, a software module has been developed to embed all these models. It allows to very quickly and very easily select most machine components key dimensions.

2 DESCRIPTION OF THE MECHANISM

A CAD drawing of the considered mechanism is presented in Fig. 1 and Fig2 is a “Joints and Loops Graph” showing the different joints (Each box stands for a joint; S: spherical, R: revolute, P: prismatic), pointing out the actuated joints (A grey box means that the joint is actuated) and describing the way the kinematic loops are arranged. One can immediatly note that the mechanism has 8 internal degrees of freedom: each link connected to neighbours by two S joints can rotate about the axis passing by the S joints centres. If needed for technological reasons, this can be

suppressed by replacing one of the S joint by a Universal joint – U Joint – ; the mechanism would then become isostatic; moreover, if hyperstatic construction is made possible by very accurate machining and assembly (or by accepting local deformations) it is even feasible to replace all S joints by U joints.

In Fig. 3a scheme, it can be seen that the proposed mechanism belongs to the Delta-Hexa "family": actuators are fixed on the base, and links of constant length are connected to the nacelle. The main interest of using spatial parallelograms lies in the fact that the bars are only stressed in tension-compression (see **[15]** for a less stiff parallel mechanism using one bar and universal joints instead of spatial parallelograms). This kind of stress is easier to manage than torsion and flexion and the consequences are a good stiffness of the whole machine.

The machine uses "pairs" of rods linking each motor to the nacelle; the key issue in designing this four-degree-of-freedom machine is to build a non-rigid nacelle to obtain the additional rotation. The shape of the articulated travelling plate looks like letter "H" where two revolute joints are located on each end of the central bar. The two lateral bars have the same behaviour as if they belong to a Delta-like robot that is to say that their possible displacements are translations only. A displacement of one lateral bar of the "H" relative to the other one produces the desired rotation about Z axis.

Here, 4 linear actuators are used; they are parallel to the longest displacement direction, so the machine is well suited to workspace specifications.

The denomination of points used in following models is introduced in Fig. 3b. The mechanism description is as follows:

- P_i is the origin of prismatic joint i belonging to chain i
- $\boldsymbol{U_i}$ is the unit vector giving the direction of the prismatic joint
- q_i is the position of actuator number i . q_i is counted positive in the direction of $\boldsymbol{U_i}$
- A_{i1} and A_{i2} are the joints centres (spherical or universal) at actuators side
- A_i is the middle of $[A_{i1}A_{i2}]$
- B_{i1} and B_{i2} are the joints centre (spherical or universal) at nacelle side
- B_i is the centre of $[B_{i1}B_{i2}]$
- $\boldsymbol{V_i}$ is the unit vector whose direction is given by $\boldsymbol{A_{i1}A_{i2}}$ (or $\boldsymbol{B_{i1}B_{i2}}$)

- d_i is equal to half the distance between A_{i1} and A_{i2} (or B_{i1} and B_{i2})

- L_i is the length of chain i rods (the rods in a given pair are supposed to have the same length)

- the union of chains 1 and 2 (respectively 3 and 4) is called “metachain 1” (respectively “metachain 2”)

- the direction of revolute joints at points C_1 and C_2 is given by vector $\boldsymbol{W}$

- the end point of the mechanism is point D

- The centre of mass of the carried object is point E .

If some geometric constraints are satisfied [**16**], the 4 degrees of freedom of the end part are three translations and one rotation about a given axis. For the presented mechanism, these constraints are:

- the bars in a pair must remain parallel and have the same length

- the chosen geometry is not always singular (For example, if all vectors $\boldsymbol{V_i}$ are parallel, the mechanism is always singular and gets one uncontrolled degree of freedom).

For internal collision avoidance at the travelling plate level, the rotation angle is limited to +/-45°. A gear amplification device with a 1:4 ratio (Fig. 4) is added to achieve a +/-180° angle.

3 POSITION RELATIONSHIPS

The relation between the actuators position ($\boldsymbol{Q} = [q_1 \quad \ldots \quad q_4]^T$) and the nacelle position ($\boldsymbol{X}$ expressed in the fixed reference frame) is derived in this section. $\boldsymbol{X}$ is expressed as $\boldsymbol{X} = [\boldsymbol{x}^T \quad q]^T$, where $\boldsymbol{x}$ is the vector composed by the Cartesian coordinates of point D in the reference frame, and q is the angle describing the rotation of $\boldsymbol{C_1C_2}$ about $\boldsymbol{W}$.

Inverse model

Only the relation giving $\boldsymbol{Q}$ as a function of $\boldsymbol{X}$ can always be computed in an analytical way whatever the mechanism arrangement is. Indeed, given $\boldsymbol{X}$, position of points C_1 and C_2 can be computed as follows:

$$\boldsymbol{C_1} = \boldsymbol{x} + \mathbf{Rot}(\boldsymbol{W},q)(\boldsymbol{DC_1})_0 \text{ and } \boldsymbol{C_2} = \boldsymbol{x} + \mathbf{Rot}(\boldsymbol{W},q)(\boldsymbol{DC_2})_0 \quad (1)$$

where $(\ )_0$ denotes the reference position.

Position of points B_i is given by:

$$\mathbf{B} = [\boldsymbol{C_1} \quad \boldsymbol{C_1} \quad \boldsymbol{C_2} \quad \boldsymbol{C_2}] + \mathbf{CB} \quad (2)$$

Given $\boldsymbol{Q}$, position of points A_i is:

$$\boldsymbol{A_i} = \boldsymbol{P_i} + q_i \boldsymbol{U_i} \quad (3)$$

That is:

$$\mathbf{A} = \mathbf{P} + \mathbf{U}\ \mathbf{diag}(\boldsymbol{Q}) \quad (4)$$

The equation between $\boldsymbol{Q}$ and $\boldsymbol{X}$ can be derived writing that length of A_iB_i is equal to L_i:

$$\boldsymbol{A_iB_i}.\boldsymbol{A_iB_i} = {L_i}^2 \quad (5)$$

That is:

$$\boldsymbol{A_iB_i} = (\boldsymbol{B_i} - \boldsymbol{P_i}) - q_i \boldsymbol{U_i} \quad (6)$$

So, for chain number i, a second order polynomial expression is obtained:

$${q_i}^2 - 2(\boldsymbol{B_i} - \boldsymbol{P_i}).\boldsymbol{U_i} q_i + (\boldsymbol{B_i} - \boldsymbol{P_i})^2 - {L_i}^2 = 0 \quad (7)$$

If the pose of the nacelle is reachable, this polynomial has 2 real roots. According to the choice of counting q_i positive in the direction of vectors $\boldsymbol{U_i}$, only the largest root of the polynomial is considered because it corresponds to the proper configuration of the mechanism.

Direct model

For some particular arrangements (for example the one presented in Fig.1), $\boldsymbol{X}$ as a function of $\boldsymbol{Q}$ can be expressed in closed form. In that case, geometrical parameters are:

$$\mathbf{P} = \begin{bmatrix} 0 & 0 & 0 & 0 \\ -p & -p & p & p \\ 0 & 0 & 0 & 0 \end{bmatrix} \quad (8)$$

$$\mathbf{U} = \begin{bmatrix} -1 & 1 & 1 & -1 \\ 0 & 0 & 0 & 0 \\ 0 & 0 & 0 & 0 \end{bmatrix} \quad (9)$$

$$(\mathbf{DC})_0 = \begin{bmatrix} 0 & 0 \\ -d & d \\ 0 & 0 \end{bmatrix} \quad (10)$$

$$\mathbf{CB} = \begin{bmatrix} -d & d & d & -d \\ 0 & 0 & 0 & 0 \\ 0 & 0 & 0 & 0 \end{bmatrix} \tag{11}$$

$$\boldsymbol{L} = L\begin{bmatrix} 1 & 1 & 1 & 1 \end{bmatrix}^T \tag{12}$$

$$\boldsymbol{W} = \begin{bmatrix} 0 & 0 & 1 \end{bmatrix}^T \tag{13}$$

With such data, the system (5) can be written as follows:

$$\begin{cases} (x + d\,\mathbf{sin}q - d + q_1)^2 + (y - d\,\mathbf{cos}q + p)^2 + z^2 = L^2 \\ (x + d\,\mathbf{sin}q + d - q_2)^2 + (y - d\,\mathbf{cos}q + p)^2 + z^2 = L^2 \\ (x - d\,\mathbf{sin}q + d - q_3)^2 + (y + d\,\mathbf{cos}q - p)^2 + z^2 = L^2 \\ (x - d\,\mathbf{sin}q - d + q_4)^2 + (y + d\,\mathbf{cos}q - p)^2 + z^2 = L^2 \end{cases} \tag{14}$$

Manipulating equations leads to:

$$\begin{cases} (x + d\,\mathbf{sin}q - d + q_1)^2 + (y - d\,\mathbf{cos}q + p)^2 + z^2 = L^2 \\ (2d - q_2 - q_1)(2x + 2d\,\mathbf{sin}q - q_2 + q_1) = 0 \\ (2d - q_3 + q_4)(2x - 2d\,\mathbf{sin}q - q_3 + q_4) = 0 \\ (2d\,\mathbf{sin}q + 2d - q_1 - q_3)(2x + q_1 - q_3) + 2y\,(2d\,\mathbf{cos}q - 2p) = 0 \end{cases} \tag{15}$$

Finally, direct geometry model is obtained for this particular arrangement:

$$\begin{cases} z = \pm\sqrt{L^2 - (x + d\,\mathbf{sin}q - d + q_1)^2 - (y - d\,\mathbf{cos}q + p)^2} \\ y = -\dfrac{(2d\,\mathbf{sin}q + 2d - q_1 - q_3)(2s + q_1 - q_3)}{2d\,\mathbf{cos}q - 2p} \\ x = \dfrac{-q_1 + q_2 + q_3 - q_4}{4} \\ q = Arc\,\mathbf{sin}\left(\dfrac{-q_1 + q_2 - q_3 + q_4}{4d}\right) \end{cases} \tag{16}$$

4 KINEMATICS ANALYSIS AND WORKSPACE EVALUATION

Kinematics analysis (that is: velocity transformation) and workspace evaluation are closely related issues for parallel mechanisms; as a matter of fact, there is a dramatic difference between “reachable” workspace, and “usable” workspace, and this difference can be taken into account thanks to kinematics relationship. Indeed, if a “reachable” location is a location where polynomial (7) has 2 real roots, a “usable” location is a “reachable” location where the machine will work properly with respect to accuracy-based or stiffness-based criteria. Such issues can be addressed at a preliminary stage by resorting to some properties of the velocity relationship.

Reachable workspace

A simple flooding technique is used to find the reachable workspace. For this method, a starting point belonging to the workspace is needed. Then, starting from an unit sphere (see Fig. 5 for a 2D example of this method), the sphere is expanded towards reaching the workspace boundaries with a given precision. Plot of Fig 5a is obtained for the selected mechanism (see appendix 1 for numerical values of its dimensions).

Well conditioned workspace.

In the Fig 6a plot, all the positions are reachable in a theoretical way, but practically some of them are singular or cannot be reached physically due to collisions between bars and actuators for example. So a “safe” subset of the reachable workspace must be selected.

Jacobian matrix $\mathbf{J}$ is used in the relation between actuators velocity $\dot{\boldsymbol{Q}}$ and nacelle velocity in the cartesian space $\dot{\boldsymbol{X}}$. This relation can be written as follows:

$$\dot{\boldsymbol{X}} = \mathbf{J}\dot{\boldsymbol{Q}} \tag{17}$$

For serial robots, the elements of matrix $\mathbf{J}$ are finite numbers because they depend on robot physical dimensions. The problem with parallel mechanisms is that the relation (17) comes from the following relation:

$$\mathbf{J_x}\,\dot{\boldsymbol{X}} = \mathbf{J_q}\,\dot{\boldsymbol{Q}} \tag{18}$$

In relation (18) $\mathbf{J_x}$ and $\mathbf{J_q}$ elements are finite numbers depending on physical dimensions of the machine, but both matrices can become singular. So minimum or maximum singular values, or determinant of $\mathbf{J}$ are not good criteria as their values can be zero or infinite in a singular point. Condition number of matrix $\mathbf{J}$ seems to be a good criteria as its possible minimum value is always equal to 1 and as it increases when the machine is close to a singular position [**17**].

To derive equation (18) , the classical property that relates the velocities, $\boldsymbol{V(}\mathrm{A}\boldsymbol{)}$ and $\boldsymbol{V(}\mathrm{B}\boldsymbol{)}$ of two points A and B belonging to the same rigid body is used:

$$\boldsymbol{V(}\mathrm{A}\boldsymbol{)} \bullet \boldsymbol{AB} = \boldsymbol{V(}\mathrm{B}\boldsymbol{)} \bullet \boldsymbol{AB} \tag{19}$$

Applying this relation to the four chains leads to:

$$\mathbf{J_x} = \left[\boldsymbol{A_i B_i}^T \quad (\boldsymbol{DC_j} \times \boldsymbol{A_i B_i}) \bullet \boldsymbol{W} \right] \tag{20}$$

and:

$$\mathbf{J_q} = \mathbf{diag}\left(\left[\boldsymbol{A_i B_i} \bullet \boldsymbol{U_i} \right] \right) \tag{21}$$

The method used to compute the “usable” workspace (that is to say well conditioned workspace) is to only keep the points that guarantee a minimal value of the selected criteria. To do that, the minimal value of the condition number on the whole reachable workspace is searched by optimisation. Then a safety coefficient is chosen: only the points where the condition number is smaller than the product of the minimal condition number by the selected coefficient are kept.

Regarding self-collisions, for the given range of variation for q (that is to say +/-45°), it is not useful to study the problem of self collisions: if the nacelle design respects some simple rules, the bars will never collide using well conditioned workspace. An example of this workspace is plotted in Fig 6b. On this plot, well conditioned workspace is more than two times smaller than the reachable workspace: this shows the importance of such a computation.

5 STATICS ANALYSIS

To design the mechanism, maximal forces have to be known: actuators forces are needed to select them, and internal forces are needed to design joints and others machine components.

Actuator forces

For a nacelle given pose and a given force, $\boldsymbol{F_{ext}}$, and torque, $\boldsymbol{M_{ext}}$, applied on it, the resulting force on the actuators $\boldsymbol{F_{mot}}$ is given by :

$$\boldsymbol{F_{mot}} = \mathbf{J}^T \begin{bmatrix} \boldsymbol{F_{ext}} \\ \boldsymbol{M_{ext}}.\boldsymbol{Z} \end{bmatrix} \tag{22}$$

A plot of maximal forces on the actuators is given in Fig 6a. This plot shows that the selected geometry and dimensions are not optimal because forces in actuators vary by a factor of four: the behaviour of the machine is far from being constant in the workspace.

Bar forces

The forces in bars are another important point for dimensioning machine components. Given that value and the desired load, convenient size and material can be found. This load is also useful to size passive joints. Until now, for geometry and kinematics modelling each spatial parallelogram was considered as a single bar. For the computation of forces in bars, bars in a spatial parallelogram must be distinguished. Each bar has ball joints at its ends, so the stress in each bar is only tension or compression along its axis (*ie* A_iB_i)

Nacelle's balance can be written as follows:

$$\begin{cases} \sum_{i=1}^{4}\sum_{j=1}^{2} f_{ij}\frac{\boldsymbol{A_{ij}B_{ij}}}{L_{ij}} = \boldsymbol{F_{ext}} \\ \sum_{i=1}^{4}\sum_{j=1}^{2} f_{ij}\frac{\boldsymbol{A_{ij}B_{ij}}}{L_{ij}} \times \boldsymbol{B_{ij}E} = \boldsymbol{M_{ext}} \\ \sum_{i=1}^{2}\sum_{j=1}^{2}\left(f_{ij}\frac{\boldsymbol{A_{ij}B_{ij}}}{L_{ij}} \times \boldsymbol{B_{ij}C}_1 \right).\boldsymbol{W} = 0 \\ \sum_{i=1}^{4}\sum_{j=1}^{2}\left(f_{ij}\frac{\boldsymbol{A_{ij}B_{ij}}}{L_{ij}} \times \boldsymbol{B_{ij}C}_2 \right).\boldsymbol{W} = 0 \end{cases} \quad (23)$$

where :

- i stands for spatial parallelogram number i, and j stands for the bar number j in this parallelogram.
- f_{ij} is the algebraic value of the stress in the considered bar
- $\boldsymbol{F_{ext}}$ and $\boldsymbol{M_{ext}}$ are acting at point E

This system is composed of 8 algebraic equations:

- 3 are related to forces
- 3 are related to torques
- 2 equations representing the fact that there is no torque around the nacelle revolute joints axis.

System of equations (23) can be written in a linear form as follows, assuming that all the bars have the same length L :

$$\mathbf{J_b} = \frac{1}{L}\begin{bmatrix} \boldsymbol{AB_{11}} & \boldsymbol{AB_{12}} & \dots & \boldsymbol{AB_{42}} \\ \boldsymbol{AB_{11}} \times \boldsymbol{B_{11}E} & \boldsymbol{AB_{12}} \times \boldsymbol{B_{21}E} & \dots & \boldsymbol{AB_{42}} \times \boldsymbol{B_{42}E} \\ (\boldsymbol{AB_{11}} \times \boldsymbol{B_{11}C_1}).\boldsymbol{W} & (\boldsymbol{AB_{12}} \times \boldsymbol{B_{12}C_1}).\boldsymbol{W} & \dots & \boldsymbol{0} \\ \boldsymbol{0} & \boldsymbol{0} & \dots & (\boldsymbol{AB_{42}} \times \boldsymbol{B_{42}C_2}).\boldsymbol{W} \end{bmatrix} \quad (24)$$

The linear system becomes :

$$\begin{bmatrix} \boldsymbol{F_{ext}} \\ \boldsymbol{M_{ext}} \\ 0 \\ 0 \end{bmatrix} = \mathbf{J_b} \begin{bmatrix} f_{11} \\ f_{12} \\ f_{21} \\ f_{22} \\ f_{31} \\ f_{32} \\ f_{41} \\ f_{42} \end{bmatrix} \tag{25}$$

Witch leads to:

$$\boldsymbol{F_b} = \mathbf{J_b^{-1}} \begin{bmatrix} \boldsymbol{F_{ext}} \\ \boldsymbol{M_{ext}} \\ 0 \\ 0 \end{bmatrix} \tag{26}$$

A plot of maximal forces in bars is presented in Fig 7b. For the selected geometry and dimensions, forces in bars are low and does not vary too much.

6 STIFFNESS ANALYSIS

It is obvious that for obtaining a good estimate of machine stiffness, a model using finite elements is needed. Nevertheless, such a model needs to know perfectly machine geometry and takes a lot of computing time. In a pre-sizing study it is better to have a simplified stiffness model taking only into account the less stiff parts. In this study, only stiffness of bars and stiffness of actuators are taken into account.

Given a force and torque on the nacelle, forces on actuators, given by equation (23) can be computed. Assuming that :

- k_a is the actuator stiffness along its direction of motion (all actuators are supposed to be identical)
- k_b is the stiffness of a bar (all bars are supposed to be identical)

Displacement of actuators $\boldsymbol{dA} = [dA_1 \quad \ldots \quad dA_4]^T$ can be written as (displacement of point A_i in direction of $\boldsymbol{U_i}$):

$$\boldsymbol{dA} = \mathbf{M}.\begin{bmatrix} \boldsymbol{F_{ext}} \\ \boldsymbol{M_{ext}}.\boldsymbol{Z} \end{bmatrix} \tag{27}$$

with:

$$\mathbf{M} = k_a.\mathbf{J}^T \tag{28}$$

The displacement of points A_{ij} in direction of $\boldsymbol{U_i}$ is:

$$\boldsymbol{dA}^* = \mathbf{T_A}.\begin{bmatrix} \boldsymbol{F_{ext}} \\ \boldsymbol{M_{ext}} \\ 0 \\ 0 \end{bmatrix} \tag{29}$$

with:

$$\boldsymbol{dA}^* = [dA_{11} \quad dA_{12} \quad \ldots \quad dA_{41} \quad dA_{42}]^T$$

$$\mathbf{T_A} = \mathbf{H_1 M H_2} \tag{30}$$

$$\mathbf{H_1} = \begin{bmatrix} 1 & 0 & 0 & 0 \\ 1 & 0 & 0 & 0 \\ 0 & 1 & 0 & 0 \\ 0 & 1 & 0 & 0 \\ 0 & 0 & 1 & 0 \\ 0 & 0 & 1 & 0 \\ 0 & 0 & 0 & 1 \\ 0 & 0 & 0 & 1 \end{bmatrix} \text{ and } \mathbf{H_2} = \begin{bmatrix} 1 & 0 & 0 & 0 & 0 & 0 & 0 & 0 \\ 0 & 1 & 0 & 0 & 0 & 0 & 0 & 0 \\ 0 & 0 & 1 & 0 & 0 & 0 & 0 & 0 \\ 0 & 0 & 0 & 0 & 0 & 1 & 0 & 0 \end{bmatrix} \tag{31}$$

On the other hand, a change of bars length $\boldsymbol{dL}$ can be written as :

$$\boldsymbol{dL} = k_b.\boldsymbol{F_b} \tag{32}$$

$$\boldsymbol{dL} = k_b.\mathbf{J_b}^{-1}.\begin{bmatrix} \boldsymbol{F_{ext}} \\ \boldsymbol{M_{ext}} \\ 0 \\ 0 \end{bmatrix} \tag{33}$$

The resulting displacement of the nacelle due to the change in bars length and actuator's position can be written by using the 8 following equations:

$$\boldsymbol{AB_{ij}}.\boldsymbol{AB_{ij}} = L_{ij}^2 \tag{34}$$

This leads to :

$$(\boldsymbol{dB_{ij}} - \boldsymbol{dA_{ij}}).\boldsymbol{AB_{ij}} = dL_{ij}.L_{ij} \tag{35}$$

Where :

- $\boldsymbol{dA_{ij}}$ is the displacement of point A_{ij}, due motors elasticity,
- $\boldsymbol{dB_{ij}}$ is the displacement of point B_{ij},
- dL_{ij} is the change in bars length due to deformation of bar number ij.

$\boldsymbol{dB_{ij}}$ can be easily found by the equations relative to small displacements:

$$\boldsymbol{dB_{ij}} = \begin{bmatrix} dx \\ dy \\ dz \end{bmatrix} + \boldsymbol{EB_{ij}} \times \begin{bmatrix} dq_x \\ dq_y \\ dq_z \end{bmatrix} + \boldsymbol{C_k B_{ij}} \times (dw_k \boldsymbol{W}) \tag{36}$$

Where:

- dx (namely dy, dz) is the displacement of point E about $\boldsymbol{x}$ axis (namely $\boldsymbol{y}$, $\boldsymbol{z}$)
- dq_x (namely dq_y, dq_z) is the rotation of the nacelle about $\boldsymbol{x}$ axis (namely $\mathbf{y}$, $\mathbf{z}$)
- dw_1 (namely dw_2) is the rotation about $\boldsymbol{W}$ of $\boldsymbol{B_1B_2}$ ($\boldsymbol{B_3B_4}$)
- $k = 1$ *for* $i \in \{1,2\}$, $k = 2$ *for* $i \in \{3,4\}$

Assuming that:

$$\boldsymbol{dX} = \begin{bmatrix} dx & dy & dz & dq_x & dq_y & dq_z & dw_1 & dw_2 \end{bmatrix}^T \tag{37}$$

$$\boldsymbol{dB} = \begin{bmatrix} \boldsymbol{dB_{11}} \\ \boldsymbol{dB_{12}} \\ \boldsymbol{...} \\ \boldsymbol{dB_{42}} \end{bmatrix} \text{ with } \boldsymbol{dB_{ij}} = \begin{bmatrix} dB_{ij,x} & dB_{ij,z} & dB_{ij,z} \end{bmatrix}^T \tag{38}$$

Equations (29) become:

$$\boldsymbol{d?} = \mathrm{M_X}\, \boldsymbol{dX} \tag{39}$$

Where:

$$\mathbf{M_X} = \begin{bmatrix} \mathbf{I_3} & \mathbf{pre}(B_{11}E) & \mathbf{pre}(B_{11}C_1).W & \mathbf{0} \\ \mathbf{I_3} & \mathbf{pre}(B_{12}E) & \mathbf{pre}(B_{12}C_1).W & \mathbf{0} \\ \mathbf{...} & \mathbf{...} & \mathbf{...} & \mathbf{...} \\ \mathbf{I_3} & \mathbf{pre}(B_{41}E) & \mathbf{0} & \mathbf{pre}(B_{41}C_2).W \\ \mathbf{I_3} & \mathbf{pre}(B_{42}E) & \mathbf{0} & \mathbf{pre}(B_{42}C_2).W \end{bmatrix} \quad (40)$$

Assuming that:

$$\mathbf{M_A} = \mathbf{diag}(AB_{ij}.U_i) \quad (41)$$

$$\mathbf{M_B} = \begin{bmatrix} ??_{11} & 0 & 0 & 0 & 0 & 0 & 0 & 0 \\ 0 & AB_{12} & 0 & 0 & 0 & 0 & 0 & 0 \\ 0 & 0 & AB_{21} & 0 & 0 & 0 & 0 & 0 \\ 0 & 0 & 0 & AB_{22} & 0 & 0 & 0 & 0 \\ 0 & 0 & 0 & 0 & AB_{31} & 0 & 0 & 0 \\ 0 & 0 & 0 & 0 & 0 & AB_{32} & 0 & 0 \\ 0 & 0 & 0 & 0 & 0 & 0 & AB_{41} & 0 \\ 0 & 0 & 0 & 0 & 0 & 0 & 0 & AB_{42} \end{bmatrix}^T \quad (42)$$

$$\mathbf{M_L} = \mathbf{diag}(L|_8) \quad (43)$$

Then equations (29) become:

$$\mathbf{M_B M_X}\, dX = \mathbf{M_A}\, dA + \mathbf{M_L}\, dL \quad (44)$$

$$\mathbf{M_B M_X}\, dX = (\mathbf{M_A T_A} + \mathbf{M_L T_L})F_{ext} \quad (45)$$

Finally:

$$dX = (\mathbf{M_B M_X})^{-1}(\mathbf{M_A T_A} + \mathbf{M_L T_L})F_{ext} \quad (46)$$

That is to say:

$$dX = \mathbf{K}.F_{ext} \quad (47)$$

Where the stiffness matrix of the machine, $\mathbf{K}$, is finally given by:

$$\mathbf{K} = (\mathbf{M_B M_X})^{-1}(\mathbf{M_A T_A} + \mathbf{M_L T_L}) \quad (48)$$

A plot of machine stiffness is shown on Fig 8a. Due to the machine geometry, the plot only concerns a (y, z) plane: the nacelle position along x axis does not influence the results. As expected from the results concerning maximal forces in actuators and bars, stiffness decreases when the nacelle comes close to the actuators plane.

7 ACCURACY ISSUES

The aim of this section is to find the influence of errors (manufacturing of parts and their assembly) on the final pose of the nacelle. To do so, it is possible to rely to the same strategy than for stiffness, and the following equation gives the error on point B_{ij} :

$$\boldsymbol{dB_{ij}} = \begin{bmatrix} dx \\ dy \\ dz \end{bmatrix} + \boldsymbol{EB_{ij}} \times \begin{bmatrix} dq_x \\ dq_y \\ dq_z \end{bmatrix} + \boldsymbol{C_k B_{ij}} \times (dw_k \boldsymbol{W}) + \boldsymbol{dB_{nac}} \tag{49}$$

Where:

- dx (namely dy , dz) is the displacement of point E about $\boldsymbol{x}$ axis (namely $\boldsymbol{y}$, $\boldsymbol{z}$)
- dq_x (namely dq_y , dq_z) is the rotation of the nacelle about $\boldsymbol{x}$ axis (namely $\boldsymbol{y}$, $\boldsymbol{z}$)
- dw_1 (namely dw_2) is the rotation about $\boldsymbol{W}$ of $\boldsymbol{B_1B_2}$ ($\boldsymbol{B_3B_4}$)
- $\boldsymbol{dB_{nac}}$ is the component of the location error of points B_{ij} due to their location error relative to the nacelle expressed in the reference frame.

Equation (42) can be written in the following linear form:

$$\boldsymbol{dB} = \mathbf{M_X}\, \boldsymbol{dX} + \boldsymbol{dB_{nac}} \tag{50}$$

With :

$$\boldsymbol{dX} = \begin{bmatrix} dx & dy & dz & dq_x & dq_y & dq_z & dw_1 & dw_2 \end{bmatrix}^T \tag{51}$$

Assuming that:

$$\mathbf{M} = \mathbf{M_B} \tag{52}$$

This leads to :

$$\mathbf{M}\left(\mathbf{M_X}\, \boldsymbol{dX} + \boldsymbol{dB_{nac}}\right) = \mathbf{M}\, \boldsymbol{dA} + \mathbf{M_L}\, \boldsymbol{dL} \tag{53}$$

$$\boldsymbol{dX} = \left(\mathbf{M} . \mathbf{M_X}\right)^{-1} \left[\mathbf{M}\left(\boldsymbol{dA} - \boldsymbol{dB_{nac}}\right) + \mathbf{M_L}\, \boldsymbol{dL}\right] \tag{54}$$

$$\boldsymbol{dX} = \mathbf{S} . \begin{bmatrix} \boldsymbol{dA} \\ \boldsymbol{dB_{nac}} \\ \boldsymbol{dL} \end{bmatrix} \tag{55}$$

where:

$$\mathbf{S} = \left(\mathbf{M}.\mathbf{M}_{\mathbf{X}}\right)^{-1}\left[\mathbf{M} \quad \mathbf{M} \quad \mathbf{M}_{\mathbf{L}}\right] \tag{56}$$

is the error sensitivity matrix.

An example of sensitivity plot is given on Fig 8b. Not surprisingly, the machine accuracy varies within the workspace. Such plots should be taken into account to select properly the machining means and the assembly process in order to reach the desired machine quality.

8 CONCLUSION

In this case study, fast handling of heavy parts is considered as a potential application field for parallel mechanisms. A new machine concept is introduced to fulfil the key requirements of such an application. The mechanisms models are derived concerning geometry, workspace, kinematics, statics, stiffness and accuracy. A software module embedding all these tools have been written. The aim of this software is to offer a tool for quick design an dimensioning of this four-degree-of-freedom parallel mechanism. An appropriate interface let the user choose dimensional parameters of the machine for a given family of arrangements. Then some additional parameters are required as steps for computations, mass of parts… . Plots of reachable workspace, well conditioned workspace, forces in actuators and bars, stiffness and accuracy are then available.

The next steps of this research will be the definition of optimisation criterions and the construction of the real prototype based on the optimised mechanism.

Acknowledgements

This work has been partially supported by the European Commission (MACH21 Project, GIRD CT1999 00150).

REFERENCES

1 **Gough, V.E.** Contribution to discussion of papers on research on automotive stability, control and tire performance. *Proc. Auto Div. Inst. Mechanical engineers*, 1956-1957.

2 **Clavel, R.** Une nouvelle structure de manipulateur parallèle pour la robotique légère, *APII*, 1989, **23**(6), 501-519.

3 Merlet, J-P.. Parallel robots. Kluwer, Dordrecht, 2000.

4 **Company, O. Pierrot, F. Launay, F.** and **Fioroni, C.** Modelling and preliminary design issues of a 3-axis parallel machine-tool. *Proc. PKM-2000 conference*, Ann Arbor, USA, 2000, 14-23.

5 **Gosselin, F.** and **Lallemand, J.-P.** A new insight into the duality between serial and parallel non-redundant and redundant manipulators. In n Robotica, 2001 vol 19-4, 365-370.

6 **Pierrot, F.** and **Company, O.** Towards non-hexapod mechanisms for high performance parallel machines. *Proc. IECON 2000*, Nagoya, 2000, Japan.

7 **Siciliano, B.** The Tricept robot: Inverse kinematics, manipulability analysis and closed-loop direct kinematics algorithm, *Robotica*, 1999, **17**, 437–445

8 **Ryu, S.J. Kim, J.W. Hwang, J.C. Park, C. Cho, H.S. Lee K., Lee Y., Cornel, U. Park, F.C.** and **Kim, J.** ECLIPSE : An Overactuated Parallel Mechanism for Rapid Machining. *Proc. ASME International Mechanical Engineering Congress and Exposition*, U.S.A, 1998 vol. 8, 681-689

9 **Marquet, F. Krut, S. Company, O.** and **Pierrot F.,** ARCHI, a redundant mechanism for machining with unlimited rotation capacities. *To appear in pour ICAR 2001, 10th International Conference on Advanced Robotics*, Budapest, Hungary, 2001.

10 **Hesselbach, J. Plitea, N. Frindt, M.** and **Kusiek, A.** A new parallel mechanism to use for cutting convex glass panels. *In ARK*, Strobl, 1998 165-174,

11 **Koevermans, W.P.** and **al.** Design and performance of the four d.o.f. motion system of the NLR research flight simulator. *In AGARD Conf. Proc. No 198, Flight Simulation*, La Haye, 1975, 17-1/17-11

12 **Rolland, L.H.** The Manta and the Kanuk novel 4-dof parallel mechanisms for industrial handling. *In ASME Int. Mech. Eng. Congress*, Nashville, 1999

13 **Tanev, T.K.** Forward displacement analysis of a three legged four-degree-of-freedom parallel manipulator. *In ARK*, Strobl, 1998, 147-154

14 **Zlatanov, D.** and **Gosselin, C.M.** A family of new parallel architectures with four degrees of freedom. *In F.C. Park C.C. Iurascu, editor, Computational Kinematics*, 2001, 57-66

15 **Tsai, L-W.** Kinematics of a three-dof platform with three extensible limbs. *In J. Lenarcic V. Parenti-Castelli, editor, Recent Advances in Robot Kinematics*, 401-410. Kluwer, 1996

16 **Pierrot, F.** and **Company, O.** H4: a new family of 4-degree of freedom parallel robots. AIM'99. *Proc. IEEE/ASME International Conference on Advanced Intelligent Mechatronics*, Atlanta, Georgia, USA, 1999, 508-513.

17 **Yoshikawa, T.** Manipulability of robotic mechanisms. *In The International Journal of Robotics Research*, vol 4-2, 1985 ,3-9

FIGURES

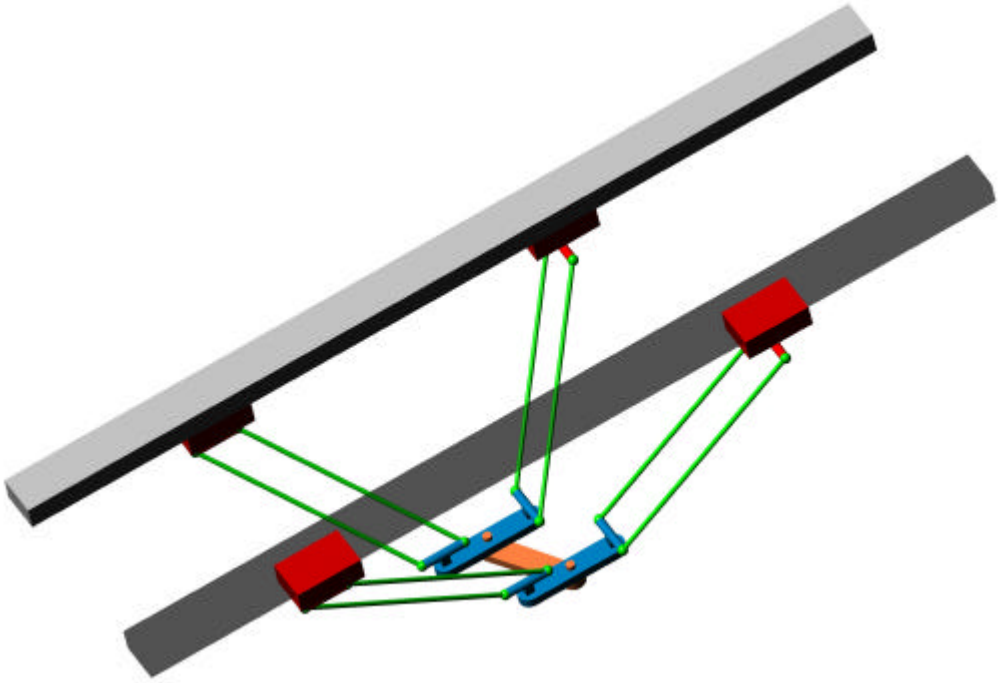

Fig. 1. Machine presentation.

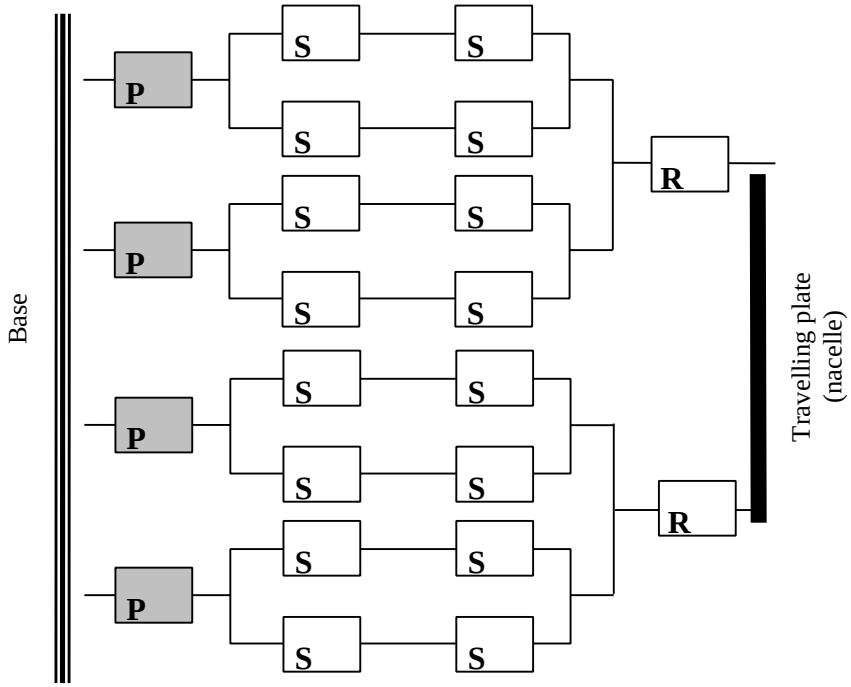

Fig. 2. Joints and Loops Graph.

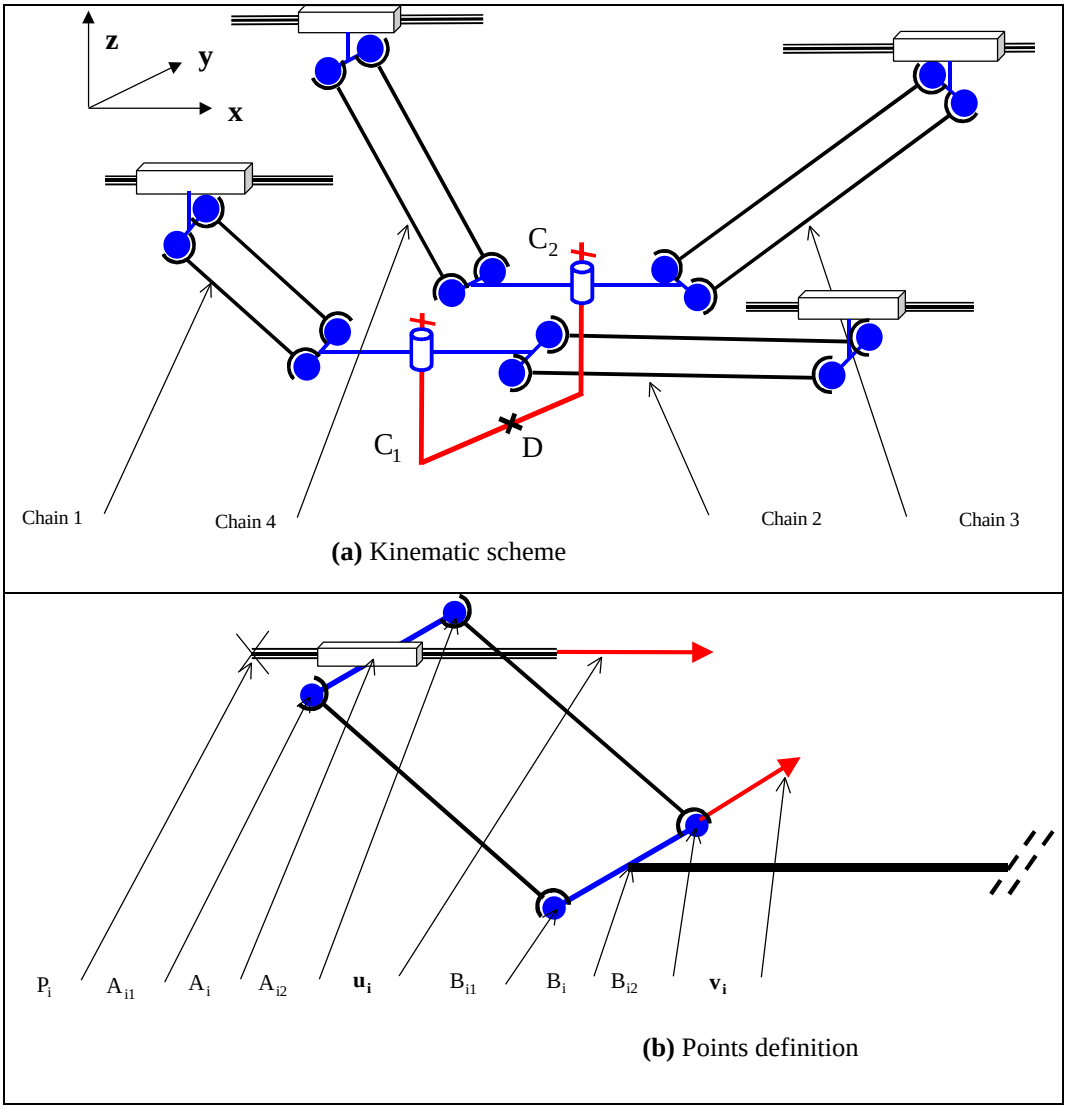

Fig. 3. Description for modelling

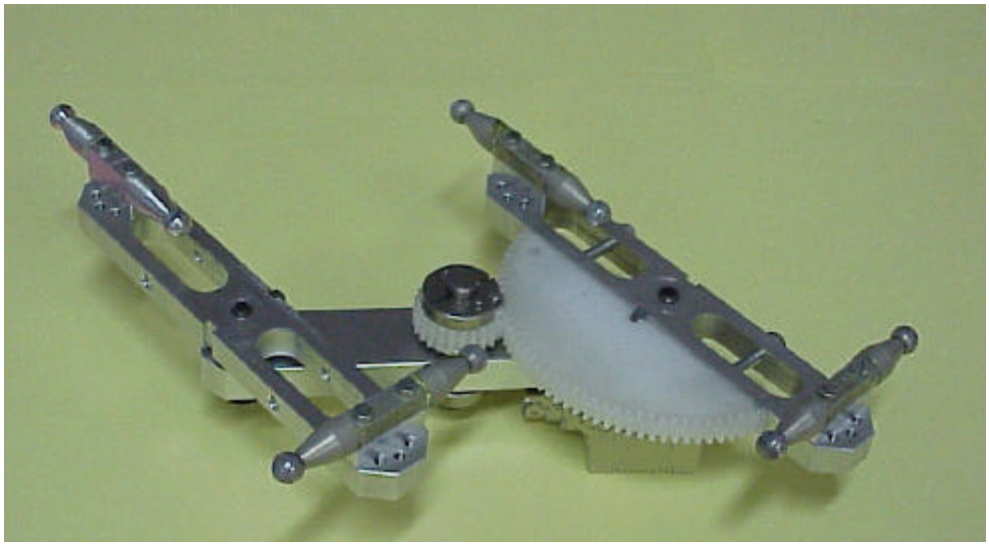

Fig. 4. A view of the gear amplification device.

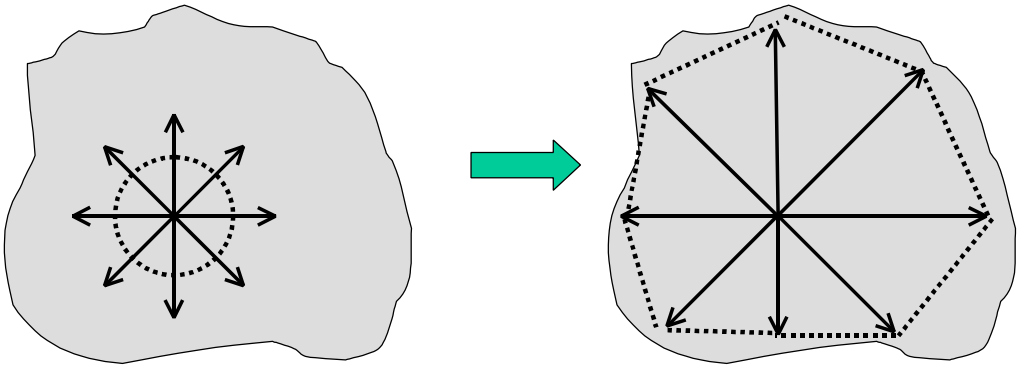

Fig. 5. Flooding technique.

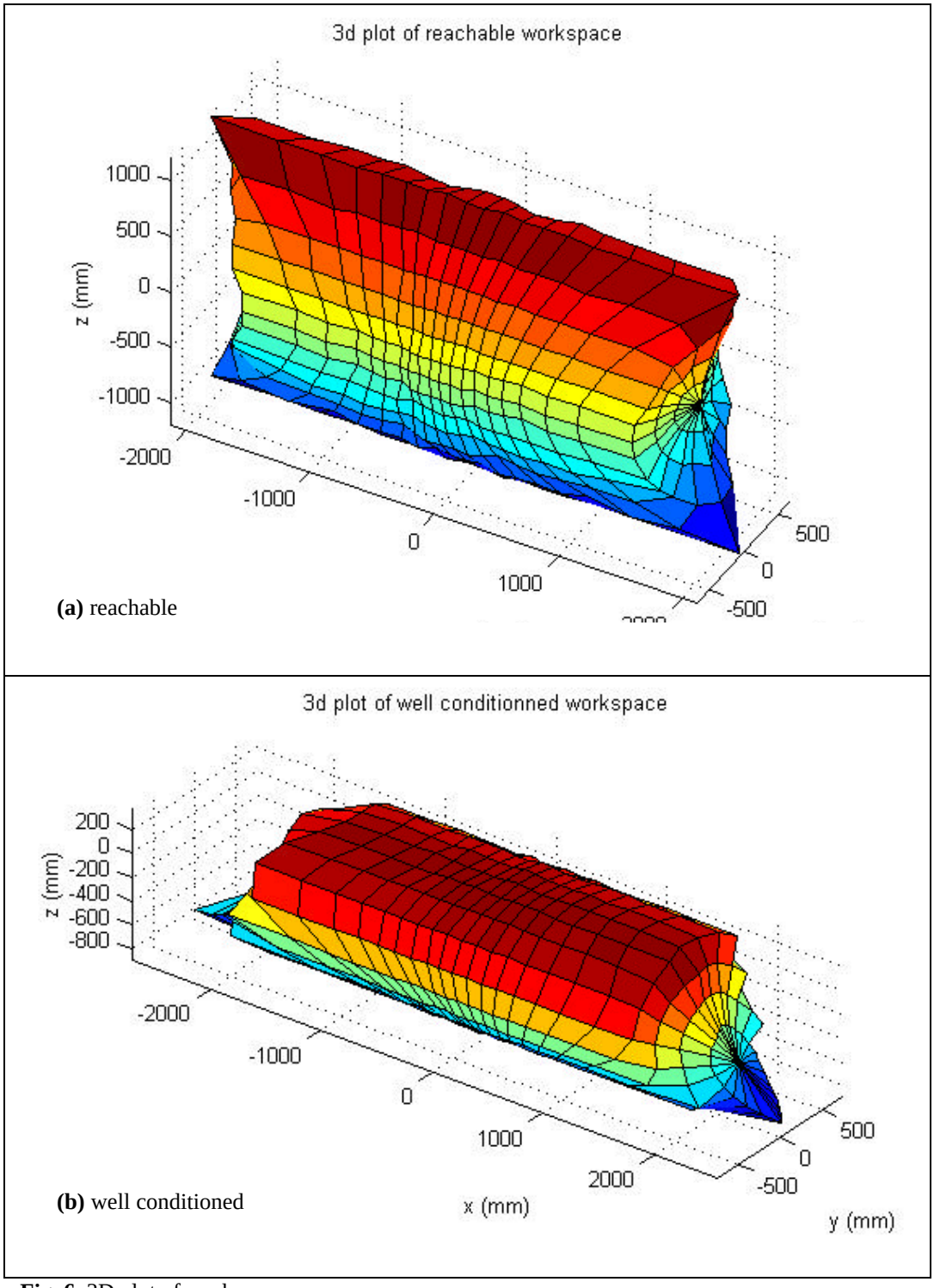

(a) reachable

(b) well conditioned

Fig. 6. 3D plot of workspace.

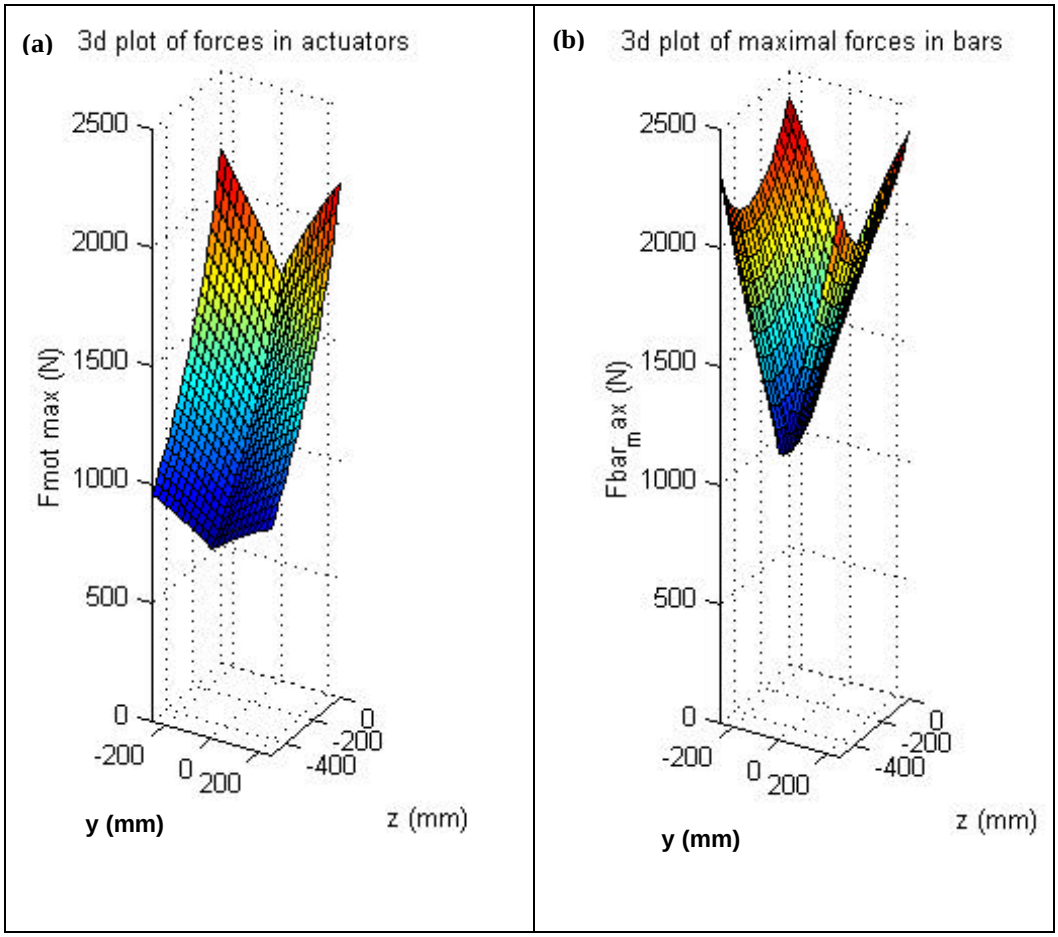

Fig. 7. Maximal forces on the actuators and on the bars.

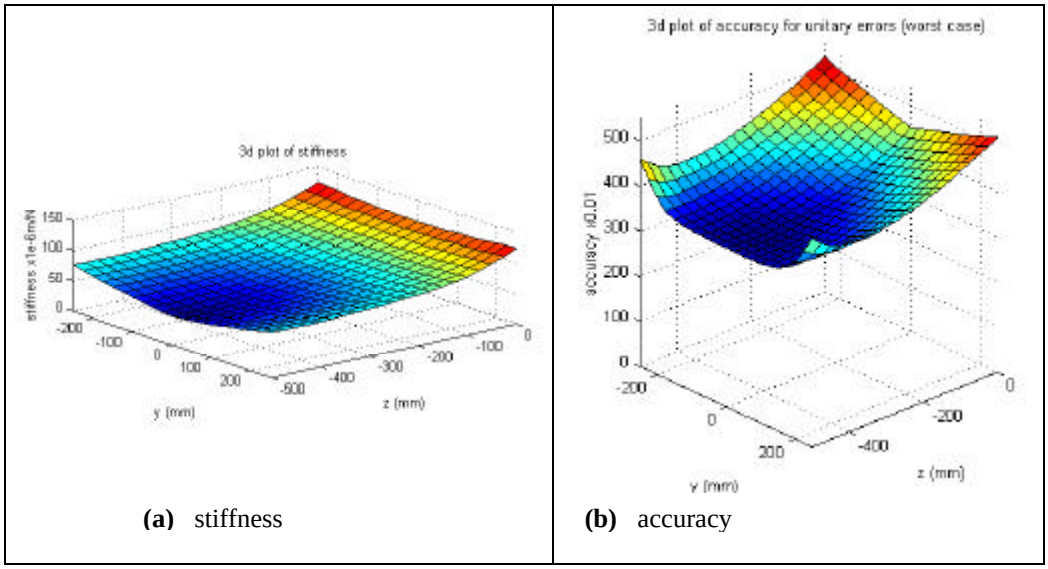

(a) stiffness **(b)** accuracy

Fig. 8. Stiffness and accuracy plots.

APPENDIX – Parameters for numerical examples

All dimensions are expressed in millimetres.

$d = 100$

$p = 700$

$L = 1500$

$$\mathbf{U} = \begin{bmatrix} -1 & 1 & 1 & -1 \\ 0 & 0 & 0 & 0 \\ 0 & 0 & 0 & 0 \end{bmatrix}$$

$$\boldsymbol{W} = \begin{bmatrix} 0 & 0 & 1 \end{bmatrix}^T$$

$$\mathbf{V} = \begin{bmatrix} 0.4615 & 0.4615 & 0.4615 & 0.4615 \\ 0.1925 & -0.1925 & 0.1925 & -0.1925 \\ 0.8660 & -0.8660 & -0.8660 & 0.8660 \end{bmatrix}$$

$\left\| \boldsymbol{B_{i1}B_{i2}} \right\| = 100$

$M_{nac} = 116kg$

Maximal acceleration for translations $\Gamma_{trans} = 5m/s^2$

Maximal acceleration for rotation $\Gamma_{rot} = 30rad/s^2$

Rotational inertia of the carried object $I_z = 0.38kgm^2$

$ED = \begin{bmatrix} 0 & 0 & 300 \end{bmatrix}^T$

Stiffness of one bar $k_b = 1e^{-5}m/N$

Stiffness of one actuator $k_a = 1e^{-4}m/N$

LIST OF CAPTIONS